Examination of Nonliquidlike Behaviors in Molten Polymer Films

Zhao H. Yang,[†] Yong J. Wang,[‡] Lela Todorova,[†] and Ophelia K. C. Tsui*,[†]

Department of Physics, Boston University, Boston, Massachusetts 02215, and Department of Physics, Hong Kong University of Science and Technology, Clear Water Bay, Hong Kong

Received July 31, 2008; Revised Manuscript Received September 14, 2008

ABSTRACT: Several experiments have shown that polystyrene (PS) films with thicknesses of $h \approx 2R_G$ (where R_G is the radius of gyration of the polymer) exhibited nonliquidlike behaviors even in the molten state. By measuring the surface spectrum of PS films subjected to different thermal annealing, we show that similar nonliquidlike behaviors can be produced if the annealing time is below $\tau(q_{lc}^{eq}(h))$, the relaxation time of the capillary wave mode with wave vector equal to the lower-cutoff wave vector $q_{lc}^{eq}(h)$, which characterizes the equilibrium surface spectrum. At the same time, annealing above $\tau(q_{lc}^{eq}(h))$ recovers the liquid behaviors. Because $\tau(q_{lc}^{eq}(h))$ often amounts to days and even years, insufficient annealing constitutes a likely cause for the nonliquidlike behaviors. Nonetheless, the previously suggested strong pinning of the polymer chains to the substrate can also be a cause. To elucidate the origin of the observed nonliquidlike behaviors, we measure the surface dynamics of PS films with $h = 2R_G$ to $8R_G$ undergoing the glass-to-rubber transition and find that they are all the same. Our result favors insufficient annealing to be the cause of the observed nonliquidlike behaviors.

Introduction

The burgeoning of nano science and technology has stimulated immense interest in the study of new materials properties brought about by nanoconfinement. For polymers under confinement in nanometer films, studies of their structural and dynamical properties have led to perplexing results. Diffuse X-ray scattering showed that polystyrene (PS) films supported by silicon, where the film thickness, h, ranged from $2R_G$ to $10R_G$ (where R_G is the radius of gyration of the polymer and typically 1−30 nm) demonstrated surface structures deviant from that of equilibrium liquid films even at temperatures well above the glass transition temperature, T_g, where the polymer should be in a molten state or, in other words, behave as a simple liquid.[1,2] At the same time, X-ray photon correlation spectroscopy (XPCS) revealed that the surface dynamics of molten PS films with $h = 2R_G$ were like those of overdamped capillary waves on a viscoelastic *solid* film,[3] albeit dynamics consistent with those of overdamped capillary waves on a simple *liquid* film were observed when $h \geq 4R_G$.[4] These results have led to the suggestion that the chain segments of PS are strongly pinned to the substrate surface, which may cause the polymer layer next to the substrate to be solidlike.[1−3] On the other hand, a large number of experiments have found that the T_g of these films decreased with decreasing h for $h < \sim 50$ nm, and unusual enhancement of the T_g was never observed as h approached $2R_G$.[5,6] In this study, we seek to reconcile the apparent inconsistency between the aforementioned X-ray and T_g measurements, which constitutes a major obstacle to the understanding of the dynamics of polymer films.[5−11]

The organization of this paper is as the following. We first show that the nonliquidlike behaviors can be interpreted by an alternative physical effect besides surface-pinning of the polymer segments. Then we examine if the dynamics of PS films with $h = 2R_G$, $4R_G$ and $8R_G$ are at all different at the glass transition by using time-resolved atomic force microscopy (AFM).[12] Time-resolved AFM has no upper limit to the experimental time-window and so allows the full course of viscoelasticity variation to be probed as the film undergoes the glass-to-rubber transition. In the end, we discuss how the findings from our measurements reconcile with previous experiments.

Experimental Section

Monodispersed PS (M_w = 2.3 to 393 kg/mol, $M_w/M_n \leq 1.16$) were purchased from Scientific Polymer Products (Ontario, NY) and used without purification. We use Si (100) subjected to a variety of surface treatments (including ones that are covered with native oxide, 5 nm thermal oxide, and no oxide) as substrates. To remove the organic contaminants, the substrates (previously cut into 1.5 × 1.5 cm^2 slides) are immersed in a solution of H_2SO_4/H_2O_2 (7:3) at 90 °C for 10 min, then thoroughly rinsed in excessive deionized water and dried with 99.99% nitrogen. If substrates with no surface oxide are desired, we start with substrates that are covered with native oxide and immerse them in an aqueous solution of 2% HF for 2 min before rinsing and drying them as above. The polymer films are prepared by spin-coating solutions of PS in toluene with concentrations 0.25−5 wt %. The film thicknesses, adjustable through the solution concentration and spinning speed, are measured by ellipsometry. Sample annealing is carried out in a sealed chamber filled with 99.99% N_2 under a slight positive pressure. To perform measurements with time-resolved AFM, we capture topographic images of the films by tapping-mode AFM at different times during annealing. To convert the topographic image into power spectral density, PSD,[12] the data is multiplied by a Welch function, followed by Fourier transformation and subsequently radial averaging. Details of the conversion procedure can be found in ref 12.

Results and Discussion

According to Frederickson et al.,[13] the equilibrium PSD of an *elastic* film with shear modulus, μ_0, is given by

$$A_q^2 = \frac{k_B T}{\gamma q^2 - \dfrac{A_{eff}}{2\pi h^4} + \dfrac{3\mu_0}{h^3 q^2}} \quad (1)$$

In eq 1, use has been made of the approximation, $qh \ll 1$, which applies to the experiments, k_B is the Boltzmann's constant, T is the absolute temperature, γ is the surface tension of PS, q is the wave vector, and A_{eff} is the effective Hamaker constant, which defines the film's van der Waals (vdW) potential, that is, $G(h) = -A_{eff}/(12\pi h^2)$.[12] (Note that the values of A_{eff} of the films studied in this work are negative and so the vdW term in eq 1 is positive.) Equation 1 differs from the result of the

* To whom correspondence should be addressed. E-mail: okctsui@bu.edu.
† Boston University.
‡ Hong Kong University of Science and Technology.

10.1021/ma801749a CCC: $40.75
Published on Web 10/09/2008

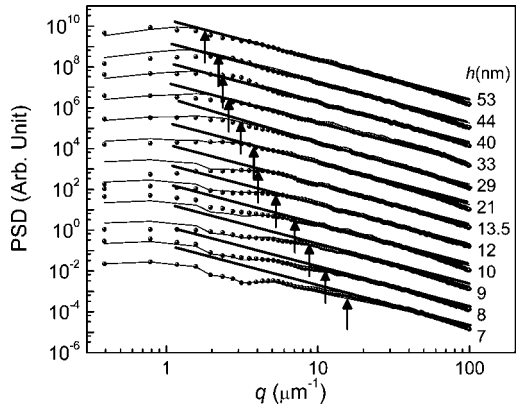

Figure 1. Log−log plots of the power spectral density of $M_w = 13.7$ kg/mol films with $7 \leq h \leq 53$ nm, spun-cast on HF-etched Si and annealed at 120 °C for 16 h. The data have been shifted vertically for clarity. The thin continuous lines are fits of the data to eq 1 plus a low-q background as described in the text. The thick lines are best fits of the model, $y = k_BT/(\gamma q^2)$ to the data in the high-q region. The ↑ arrows indicate the positions of the lower-cutoff wave vectors.

classical capillary wave theory, which applies to simple *liquid* films[14,15] by the presence of the $3\mu_0/h^3q^2$ term. This term accounts for the elastic energy required to stretch the polymer chains in the brush in order to produce the (sinusoidal) surface topography given the wave vector and equilibrium amplitude. As expected, it vanishes if $\mu_0 = 0$, as in liquids. According to eq 1, the PSD is suppressed below a lower-cutoff wave vector, q_{lc}, whose functional form depends on the relative magnitudes of the vdW and elastic energy terms in the denominator of eq 1. If the vdW term dominates (pertinent to μ_0 being small or zero), one may deduce q_{lc} by setting the first two terms in the denominator of eq 1 equal, which gives

$$q_{lc} = [-A_{eff}/(2\pi\gamma h^4)]^{1/2} \quad (2)$$

However, if the elastic energy term dominates, q_{lc} can be obtained by setting the first and third terms of the denominator of eq 1 equal, which leads to

$$q_{lc} = [3\mu_0/(\gamma h^3)]^{1/4} \quad (3)$$

The scaling of q_{lc} with respect to h, as predicted by these equations, has been used[1,2] to evaluate the liquidlike behaviors (i.e., $q_{lc} \sim h^{-2}$) or nonliquidlike behaviors (i.e., $q_{lc} \sim h^{-\beta}$, $\beta < 2$). On the other hand, it has been shown[12] that for simple liquid films (for which $\mu_0 = 0$ as with PS in the terminal flow regime), if the films are undergoing thermal equilibration, they also exhibit surface spectra consistent with eq 1; alias in that case $\mu_0 \equiv \eta/(2t)$,[12] where η is the viscosity of the film at the experimental temperature and t is the equilibration (or annealing) time. This suggests that liquid films subjected to the same thermal annealing condition but not equilibrated should also demonstrate the nonliquidlike behaviors.

We verify this prediction by measuring the lower-cutoff wave vectors of PS films with $M_w = 13.7$ kg/mol and $7 \leq h \leq 53$ nm deposited on HF-etched silicon upon annealing at 120 °C for 16 h. The PSD of these films are displayed in Figure 1. As seen, almost all the PSD curves display a distinctive kink, which is anticipated from the suppression of the PSD below q_{lc} discussed above. Seo et al.[2] determined the position of q_{lc} by fitting straight lines to portions of the PSD just above and below the kink and noting their intersection. In here, the PSD of the two thinnest films do not have a well defined region below the kink where one may obviously fit the data to a single straight line; on the other hand, variations in the choice of this fitted region can produce a significant variation in the measured value of q_{lc}. Therefore, we determine q_{lc} from the intersection between

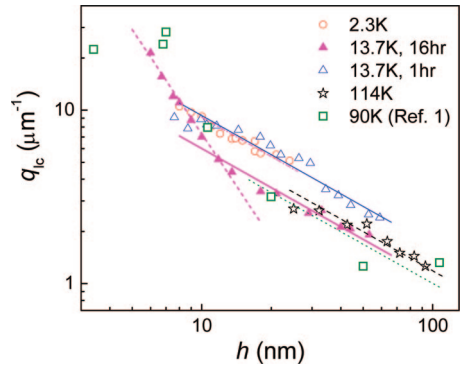

Figure 2. Log−log plot of q_{lc} versus h for PS films with various molecular weights shown in the legend. The open squares are data reproduced from ref 1. Straight lines passing through individual data are fits either to eq 2 or eq 3, as described in the text. For the latter, because $\mu_0 \equiv \eta/(2t)$, values of η can be deduced from the fits.

the PSD and the best fit of the data in the high-q region to the line, $y = k_BT/(\gamma q^2)$, with γ being the only fitted parameter and T is kept equal to the experimental annealing temperature. The reason for the choice of the fitted model (i.e., $y = k_BT/(\gamma q^2)$) is because it is the asymptotic form of eq 1 at high q. This way of determining q_{lc} may introduce a systematic error. However, it avoids random errors that can be very large. The positions of q_{lc} hence determined are indicated by the ↑ arrows in Figure 1. We have also fitted the entire series of PSD to eq 1 plus a low-q background, $A_q^2(t = 0)\Theta(q^* - q)$, where $\Theta(q^* - q)$ is the Heaviside step function and q^* is the wave vector at which the relaxation time, $\tau(q)$, of the overdamped capillary mode equals the annealing time, t. The theoretical origin of the low-q background can be found in ref 12. Physically, because the capillary modes in this region (with $q < q^*$) have relaxation times longer than t, they essentially remain stagnant during the annealing. This causes the $q < q^*$ segment of the initial PSD to persist as a low-q background. In performing the fits, we substitute μ_0 in eq 1 by $\eta/(2t)$ then fit the data by allowing only η to vary while keeping the other parameters equal to the experimental or literature values (i.e., $\gamma = 0.03$ J/m^2 and $A_{eff} = -10.6 \times 10^{-20}$ J).[16,17] The resultant model curves are displayed by the thin solid lines in Figure 1, which clearly describe the data very well. The measured q_{lc} are plotted versus h in log−log scale in Figure 2 (solid triangles). As seen, the data fall into two distinctive lines about a transition thickness, $h^* \approx 12$ nm. For $h < 12$ nm, the data display the (liquidlike) $\sim h^{-2}$ dependence (thick dashed line). By fitting the data in this region to eq 2, we deduce that $A_{eff} = (-10.1 \pm 0.20) \times 10^{-20}$ J, which agrees very well with the theoretical value.[16,17] For $h > 12$ nm, the data fit well to the (nonliquidlike) $q_{lc} \sim h^{-3/4}$ dependence (thick solid line). We examine if the observed crossover between the liquidlike and nonliquidlike behaviors at $h^* \approx 12$ nm can be explained by the present model. It can be shown that if $t \ll 6\pi^2\eta\gamma h^5/A_{eff}^2$ (which equals $\tau(q_{lc}^{eq}) = 3\eta/(2\gamma h^3 q_{lc}^4)$),[12,18] that is, the relaxation time of the surface capillary mode with $q = q_{lc}^{eq}$, the equilibrium lower-cutoff wavevector given by eq 2), the $3\mu_0/(h^3q^2)$ term dominates the vdW term in eq 1 (with $\mu_0 \equiv \eta/(2t)$), whereby the nonliquidlike $q_{lc} \sim h^{-3/4}$ dependence should prevail. As a result, with a given annealing time t, a crossover between the liquidlike and nonliquidlike behaviors would occur if $\tau(q_{lc}^{eq}(h^*) = t$. This gives

$$h^* = [A_{eff}^2 t/(6\pi^2\eta\gamma)]^{1/5} \quad (4)$$

By putting $A_{eff} = -10.6 \times 10^{-20}$J, $t = 16$ h, $\eta = 8.25 \times 10^5$ Pas (see Table 1) and $\gamma = 0.03$ J/m^2 in eq 4, we estimate that $h^* = 13$ nm, which agrees very well with the observed value of h^* (= 12 nm). The discrepancy between the observed and

Table 1. Experimental and Fitted Parameters Pertinent to the Data Shown in Figure 3

M_w (Kg/mol)	M_w/M_n	R_G (nm)	$T_{g,bulk}$ (°C)	d_{SiOx}[b] (nm)	T (°C)	t (hr)	$\eta_{literature}$[c] (10^5 Pas)	η[d] (10^5 Pas)	η[e] (10^5 Pas)
2.33	1.06	1.3	64	5	85	1	1.66	(4.9 ± 0.3)	1.5
13.7	1.10	3.1	90	0	120	1	8.25	(5.4 ± 1.1)	4.0
13.7	1.10	3.1	90	0	120	16	8.25	(15 ± 2)	4.0
114	1.08	9.1	100	2	150	12	3.91	(17 ± 3)	12
90[a]		8.0[a]	~100[a]	0	150[a]	12[a]	1.87	(8.7 ± 9.2)	NA

[a] Quotation from ref 1. [b] d_{SiOx} denotes the thickness of the oxide layer on the substrate. [c] η from ref 19. [d] η from fits to eq 3. [e] η from fits to eq 1, plus a low-q background.

estimated values of h^* can be traced to the discrepancy between the viscosity of the films as implied by the data in the $h > h^*$ region (to be discussed below) and the literature value, $\eta_{literature}$.

We have also measured q_{lc} for PS films with other molecular weights, substrate surface conditions, and thermal annealing as summarized in Table 1. The measurement results as well as the data reproduced from ref 1 are displayed in Figure 2, together with the (solid triangle) data just discussed. We have estimated the value of h^* for each data series shown in Figure 2 by applying the respective literature or experimental values to the parameters contained in eq 4 (results not shown). We find that all the estimated values of h^* deduced from our data fall below 8.3 nm (except for the solid triangle data just discussed, which have $h^* = 12$ nm) but is 12.3 nm for the films studied in ref 1. These estimates corroborate very well with the fact that our data only exhibit the $q_{lc} \sim h^{-3/4}$ dependence, whereas there is an apparent onset of the $q_{lc} \sim h^{-2}$ dependence below ~12 nm in the data of ref 1 (i.e., the open squares shown in Figure 2).

Next, we fit each data series in Figure 2 in the thickness region above the respective h^* to eq 3 with $\mu_0 \equiv \eta/(2t)$ and η treated as the only fitting parameter. The resulting model lines are the straight lines passing through individual data sets. The values of η obtained from the fits are shown in the second last column of Table 1. We have also fitted the entire series of PSD curves like those shown in Figure 1 directly to eq 1 plus a low-q background, again with $\mu_0 \equiv \eta/(2t)$ and η treated as the only fitting parameter. The fitted values of η are given in the last column of Table 1. As seen, the values of η based on fittings to eq 1 agree within a factor of ~2 with the literature values, whereas those from the fittings based on eq 3 demonstrate on average an ~30% bigger discrepancy (Table 1). The latter is understandable to be due to the additional measurement uncertainty of q_{lc}. Because the discrepancies found here are comparable to those typically found in viscosity measurements of polymers,[3] we conclude that the measured viscosities of the films are the same as those of the bulk. We explain that this conclusion is consistent with previous findings about the T_g of the films.[5,6,8,11] By measuring the cooling rate dependence of the T_g of PS supported films, Fakhraai et al.[20] showed that the large thickness-variation of T_g conventionally observed could only be found in measurements subjected to slow cooling rates (~1 °C/min); as the cooling rate was increased, the thickness variation of T_g diminished considerably. Upon a threshold cooling rate (>130 °C/min) corresponding to $T \approx T_{g,bulk} + 8$ °C), the T_g of all the films studied ($5.5 \le h \le 90$ nm) collapsed to $T_{g,bulk}$ (i.e., the T_g of the polymer in bulk). For the data shown in Figure 2, the annealing temperatures are more than 8° above the respective $T_{g,bulk}$ (Table 1). The current finding that the viscosities of the films are the same as the bulk is expected indeed.

Seo et al.[2] have observed the nonliquidlike behaviors, $q_{lc} \sim h^{-\beta}$, $0.6 \le \beta \le 1$ in PS films with $M_w = 123-900$ kg/mol and $h \ge 2R_G$ even after the films were annealed at 165 °C for over 90 h. Lacking information about the precise annealing times, one cannot apply the present model to these results. Nevertheless, we note that because the minimum annealing time required for the liquid behavior to be observed increases with increasing h and η (recall that this time is $\tau(q_{lc}^{eq}(h)) \sim \eta h^5$). As the molecular weight of the polymer used is increased, the required time can increase quickly to prohibitively large values. Take the cases focused upon in ref 2 as an example, that is, $T = 165$ °C and $h = 2R_G$, we estimate that $\tau(q_{lc}^{eq}(2R_G)) \approx 5$ d for $M_w = 200$ kg/mol, but increases rapidly to 12 yr for $M_w = 650$ kg/mol. It follows that, for the samples with $M_w > \sim 200$ kg/mol, it would be difficult to discern if the nonliquidlike behaviors are extrinsic, arising from the mechanism proposed here, or intrinsic, arising from surface pinning of the polymer segments.

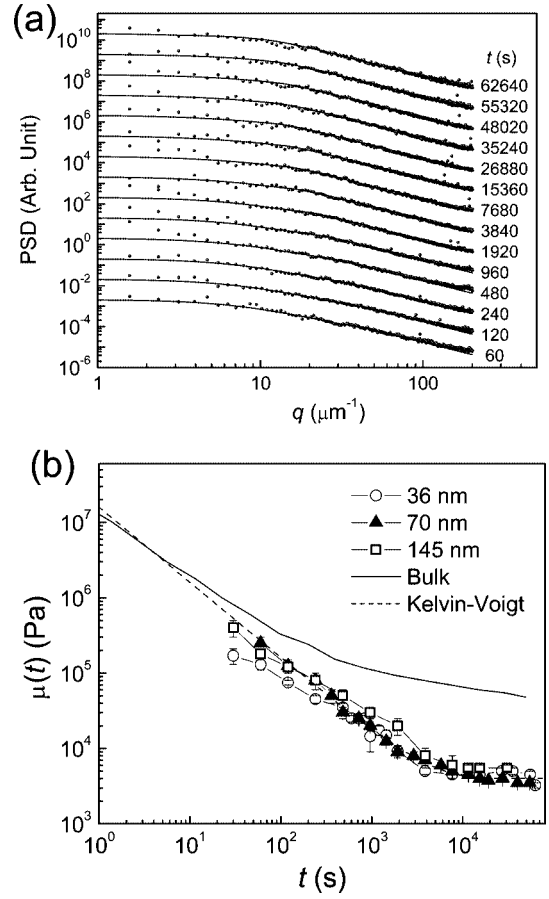

Figure 3. Data illustrating the surface dynamics of thin films of PS with $M_w = 393$ kg/mol ($R_G = 17$ nm) during annealing at 107 °C. (a) Time-sequenced PSD of an $h = 36$ nm film. The data, represented by solid circles, have been shifted vertically for clarity. The solid lines are fits to eq 1 plus a low-q background. (b) Plots of μ_0 versus t in log−log scale. The symbols are data obtained from PS films ($M_w = 393$ kg/mol) with thicknesses as stipulated in the legend. The dashed line represents the least-squares fit of the Kelvin−Voigt model to the data. The solid line is data derived from ref 21 for bulk PS with a comparable molecular weight.

To shed some light, we compare the dynamics of PS ($M_w = 393$ kg/mol, $R_G = 17$ nm) films with $h \approx 2R_G$, $4R_G$, and $8R_G$ near the glass transition. Figure 3a shows a sequence of PSD obtained from a 36 nm film annealed at 107 °C (solid circles). We fit each PSD to eq 1 by treating μ_0 (which represents the time-dependent shear modulus in the present context of dynamic glass transition) as the only fitting parameter. The hence deduced

values of μ_0 at different t together with those obtained from the $h = 70$ and 145 nm films are shown in Figure 3b. Evidently, the data of all three films look the same, namely, they all decline with t but come to a plateau after about 4000 s. We find that the data can be described quite well by the Kelvin−Voigt model, $\mu_0(t) = \mu_0/[1 - \exp(-\mu_0 t/\eta)]$, which is commonly used to describe the dynamic behavior of viscoelastic solids. From the fit of this model to our data (dashed line), we deduce that $\mu_0 =$ 4000 Pa and $\eta = 1.6 \times 10^7$ Pas. The data of bulk PS with a comparable molecular weight of 400 kg/mol[21] is also shown for comparison (solid line). It clearly demonstrates the same short-time behavior as the films, but at long times, it displays a plateau modulus μ_0 that is ~100 times that of the films. This latter finding has been observed in previous experiments[2,12] and suggested[12] to be a result of the spin-coating process that can lead to a smaller degree of chain entanglements in the films than in the bulk. Based on the agreement in the short-time behavior (Figure 3b), we deduce that the dynamics of all three films are the same as the bulk at the glass transition. This result evidences that surface pinning of the chains, if any, has insignificant influence on the dynamics of nanoconfined polymer films at the glass transition. This assertion is in keeping with the above finding that the viscosities of the films are the same as the bulk despite the substrates used possessing different surface conditions (Table 1), which should have produced different surface pinning.

Lastly, we compare the viscoelasticity displayed in Figure 3b with that observed by XPCS in ref 3, where the films have $h = 2R_G$ and $M_w = 400$ kg/mol. In XPCS,[3] viscoelasticity was characterized by the surface capillary relaxation times, τ, displaying the dependence, $\tau(q) = \tau_{Liq}(q)/[1 + \tau_{Liq}(q)(\mu_0/\eta)]$, where $\tau_{Liq}(q)$ is the relaxation time of the overdamped capillary mode with wave vector q if the film were simple liquid. This form, like the Kelvin−Voigt model, describes a viscoelastic material that exhibits the liquid character, $\tau(q) \approx \tau_{Liq}(q)$ at short times ($t \ll \eta/\mu_0$), but the solid character, $\tau(q) \approx \eta/\mu_0$ at long times ($\gg \eta/\mu_0$). In ref 3, the characteristic time, η/μ_0 was seen to scatter about a constant value ≈400 s for temperatures between 176 and 224 °C. By using the time−temperature superposition,[19,21] $\eta/\mu_0 \approx 400$ s at 224 °C corresponds to ~6 $\times 10^7$ s at 107 °C. The fact that this time far exceeds the characteristic time of ~4000 s found here for the glass transition at 107 °C suggests that the viscoelasticity revealed in ref 3 is due to a novel liquid-to-solid transition different from the glass transition. While it is tempting to relate the nonliquidlike behaviors to the solid phase of this transition,[3] there is insufficient ground to draw the connection as that would require knowledge about the as yet unknown phase diagram of this transition in the temperature range where the nonliquidlike behaviors were observed.

Conclusions

In summary, we have examined the nonliquidlike behaviors previously reported in molten polymer films. We showed that similar nonliquidlike behaviors can be produced if the preannealing time of the film is less than $\tau(q_{lc}^{eq}(h))$, the relaxation time of the capillary wave mode with $q = q_{lc}^{eq}(h)$, the lower-cutoff wave vector of the film at equilibrium. The fact that $\tau(q_{lc}^{eq}(h))$ are often on the order of days and even years makes insufficient annealing a probable cause of the nonliquidlike behaviors, besides strong adsorption of the polymer segments to the substrate. We also measured the surface dynamics of PS films with $h = 2R_G$, $4R_G$, and $8R_G$ at the glass-to-rubber transition and found that they were all the same. This result is consistent with previous measurements of the T_g of polymer films, where no anomalous enhancement was ever observed near $h = 2R_G$ and favors insufficient annealing to be the cause of the observed nonliquidlike behaviors.

Acknowledgment. O.K.C.T. is grateful to the support of NSF (Project No. DMR-0706096) and ACS Petroleum Research Fund (Project No. 47882-AC 5). L.T. acknowledges the support by Boston University through the UROP program.

References and Notes

(1) Wang, J.; Tolan, M.; Seeck, O. H.; Sinha, S. K.; Bahr, O.; Rafailovich, M. H.; Sokolov, J. *Phys. Rev. Lett.* **1999**, *83*, 564–567.
(2) Seo, Y. S.; Koga, T.; Sokolov, J.; Rafailovich, M. H.; Tolan, M.; Sinha, S. *Phys. Rev. Lett.* **2005**, *94*, 157802.
(3) Jiang, Z.; Kim, H.; Jiao, X.; Lee, H.; Lee, Y.-J.; Byun, Y.; Song, S.; Eom, D.; Li, C.; Rafailovich, M. H.; Lurio, L. B.; Sinha, S. K. *Phys. Rev. Lett.* **2007**, *98*, 227801.
(4) Kim, H. J.; Rühm, A.; Lurio, L. B.; Basu, J. K.; Lal, J.; Lumma, D.; Mochrie, S. G. J.; Sinha, S. K. *Phys. Rev. Lett.* **2003**, *90*, 068302.
(5) Keddie, J. L.; Jones, R. A. L.; Cory, R. A. *Europhys. Lett.* **1994**, *27*, 59–64.
(6) Forrest, J. A.; Dalnoki-Veress, K. *Adv. Colloid Interface Sci.* **2001**, *94*, 167–196.
(7) van Zanten, J. H.; Wallace, W. E.; Wu, W.-L. *Phys. Rev. E* **1996**, *53*, R2053–R2056.
(8) Baschnagel, J.; Varnik, F. *J. Phys.: Condens. Matter* **2005**, *17*, R851–R953.
(9) Alcoutlabi, M.; McKenna, G. B. *J. Phys.: Condens. Matter* **2005**, *17*, R461–R524.
(10) Roth, C. B.; Dutcher, J. R. *J. Electroanal. Chem.* **2005**, *584*, 13–22.
(11) Tsui, O. K. C. *Polymer Thin Films*; World Scientific: Singapore, 2008; Ch. 11, publication pending.
(12) Tsui, O. K. C.; Wang, Y. J.; Lee, F. K.; Lam, C.-H.; Yang, Z. *Macromolecules* **2008**, *41*, 1465–1468.
(13) Fredrickson, G. H.; Ajdari, A.; Leibler, L.; Carton, J.-P. *Macromolecules* **1992**, *25*, 2882–2889.
(14) Sanyal, M. K.; Sinha, S. K.; Huang, K. G.; Ocko, B. M. *Phys. Rev. Lett.* **1991**, *66*, 628–631.
(15) Sferrazza, M.; Xiao, X.; Jones, R. A. L.; Bucknall, D. G.; Webster, J.; Penfold, J. *Phys. Rev. Lett.* **1997**, *78*, 3693–3696.
(16) Zhao, H.; Wang, Y. J.; Tsui, O. K. C. *Langmuir* **2005**, *21*, 5817–5824.
(17) The Hamaker constant of Si and PS is -23 and -6.69×10^{-20} J, respectively.[16] By using the combining relation,[16] we obtain $A_{eff} = -10.6 \times 10^{-20}$ J.
(18) Jiang, Z.; Kim, H.; Mochrie, S. G. J.; Lurio, L. B.; Sinha, S. K. *Phys. Rev. E* **2006**, *74*, 011603.
(19) Majeste, J.-C.; Montfort, J.-P.; Allal, A.; Marin, G. *Rheol. Acta* **1998**, *37*, 486–499.
(20) Fakhraai, Z.; Forrest, J. A. *Phys. Rev. Lett.* **2005**, *95*, 025701.
(21) Strobl, G. R. *The Physics of Polymers*; Springer-Verlag: Berlin, Germany, 1996.

MA801749A